

Paleoclimate reconstruction in the Levant region

C. Nehme et al.

Paleoclimate reconstruction in the Levant region from the petrography and the geochemistry of a MIS 5 stalagmite from the Kanaan Cave, Lebanon

C. Nehme^{1,2}, S. Verheyden^{1,2}, S. R. Noble³, A. R. Farrant⁴, J. J. Delannoy⁵, and P. Claeys²

¹Department of Earth and History of Life, Royal Institute of Natural Sciences (RBINS), Brussels, Belgium

²Analytical, Environmental & Geo-Chemistry, Department of Chemistry, Faculty of Sciences Vrije Universiteit Brussel, Belgium

³British Geological Survey, Keyworth, Nottingham, NG12 5GG, UK

⁴NERC Isotope Geochemistry Laboratory, Keyworth, Nottingham, NG12 5GG, UK

⁵Laboratoire EDYTEM UMR 5204 CNRS, Université de Savoie Mont-Blanc, Pôle Montagne, Bourget-du-Lac, France

Title Page

Abstract

Introduction

Conclusions

References

Tables

Figures



Back

Close

Full Screen / Esc

Printer-friendly Version

Interactive Discussion



Received: 17 June 2015 – Accepted: 25 June 2015 – Published: 17 July 2015

Correspondence to: C. Nehme (carole.nehme@naturalsciences.be)

Published by Copernicus Publications on behalf of the European Geosciences Union.

CPD

11, 3241–3275, 2015

**Paleoclimate
reconstruction in the
Levant region**

C. Nehme et al.

Title Page

Abstract

Introduction

Conclusions

References

Tables

Figures



Back

Close

Full Screen / Esc

Printer-friendly Version

Interactive Discussion



Abstract

Lying at the transition between the temperate Mediterranean domain and subtropical deserts, the Levant is a key area to study the palaeoclimatic response over glacial-interglacial cycles. This paper presents a precisely dated last interglacial (MIS 5) stalagmite (129–84 ka) from the Kanaan Cave, Lebanon. Variations in growth rate and isotopic records indicate a warm humid phase at the onset of the last interglacial at ~ 129 ka that lasted until ~ 125 ka. A gradual shift in speleothem isotopic composition (125–122 ka) is driven mainly by the $\delta^{18}\text{O}$ source effect of the Eastern Mediterranean surface waters during Sapropel S5. The onset of glacial inception began after ~ 122 ka, interrupted by a short wet pulse during Sapropel S4. Low growth rates and enriched oxygen and carbon values until ~ 84 ka indicate a transition to drier conditions during Northern Hemisphere glaciation.

1 Introduction

Located at the interface between mid and high latitude climate systems, and affected by both the North Atlantic Oscillation and the monsoonal system over Africa, the Levant region (East Mediterranean Basin) has the unique potential to record the occurrence of climatic changes in both systems. Known for its long record of prehistoric human settlements, the Levant straddles the transition zone between the more humid Mediterranean climate in the north and the arid Saharo-Arabian desert climate regime in the south. This transition zone is characterised by steep precipitation and temperature gradients. Over the past decade, several studies have attempted to understand the palaeoclimate of this critical region (Fig. 1a) using both marine (Kallel et al., 1997; Rossignol-Strick et al., 1999; Emeis et al., 2003) and continental paleoclimate records (Frumkin et al., 2000; Bar-Mathews et al., 2003; Kolodny et al., 2005; Develle et al., 2011; Ayalon et al., 2013; Vaks et al., 2013; Gasse et al., 2015). A key period for understanding the climate system in the Levant is the last interglacial; Marine Isotope Stage (MIS) 5. This

CPD

11, 3241–3275, 2015

Paleoclimate reconstruction in the Levant region

C. Nehme et al.

Title Page

Abstract

Introduction

Conclusions

References

Tables

Figures



Back

Close

Full Screen / Esc

Printer-friendly Version

Interactive Discussion



is generally considered to be a warm period, comparable to the present-day climate, although this is still under considerable debate (Vaks et al., 2003; Lisker et al., 2010; Ayalon et al., 2011, 2013; Bar-Mathews et al., 2014). However, discrepancies between different palaeoclimate archives exist, particularly between speleothem and lacustrine archives. In particular, inconsistencies between records from Negev desert (Vaks et al., 2003, 2006), central Israel/Palestine (Bar-Mathews et al., 2000, 2003; Frumkin et al., 2000) and Lebanon (Develle et al., 2011; Gasse et al., 2011, 2015); and between the eastern Mediterranean coastline (Ayalon et al., 2013) and inner basins (e.g. Dead Sea Basin) (Kolodny et al., 2005; Enzel et al., 2008; Lisker et al., 2010) are evident. In particular, speleothem isotopic records of Soreq, Peqiin and West Jerusalem caves suggest the interglacial optimum was wet, but low lake levels in the Dead Sea basin are indicative of drier conditions during the same period.

Whereas these different continental records reflect changes in atmospheric circulation, regional topographic patterns and/or site-specific climatic and hydrological factors, the lack of detailed, accurately dated long-term records from the northern Levant, especially from different continental archives, limits our understanding of the regional response to climatic conditions during MIS 5. This lack of data restricts the opportunities to resolve the inconsistencies between paleoclimate records across the region. This study attempts to resolve this by providing a new high-resolution record obtained from a speleothem from a cave in the northern Levant. Speleothems are secondary chemical cave deposits, which provide high-resolution proxy tools for paleoclimate reconstruction (Genty et al., 2001; Drysdale et al., 2007, 2009). Recent studies highlight the significance of speleothem records, in particular for achieving precise chronologies of continental climate changes (Wang et al., 2001; Fairchild et al., 2006; Genty et al., 2003, 2006; Cheng et al., 2009). In this paper, we examine the petrography, growth history and stable isotope geochemistry of a stalagmite from Kanaan cave, situated close to the Mediterranean coast on the western flank of Mount Lebanon near Beirut, Lebanon. This speleothem provides a precise U–Th dated continental record of climate

CPD

11, 3241–3275, 2015

Paleoclimate reconstruction in the Levant region

C. Nehme et al.

Title Page

Abstract

Introduction

Conclusions

References

Tables

Figures



Back

Close

Full Screen / Esc

Printer-friendly Version

Interactive Discussion



history from the northern Levant spanning the last interglacial and the glacial inception of this region.

2 Climate and paleoclimatic setting

Lebanon is located in the northern Levant between latitudes 32°34' N and 34°41' N (Fig. 1). The western side of the country is characterized by a Mediterranean climate with an annual precipitation varying between 880 and 1100 mm along the coastline (World Bank, 2003). The climate is seasonal; with wet winters (between November and February) and dry, hot summers (from May to October). The present climate is influenced by the Atlantic Westerlies, which bring in moist winds associated with extra-tropical cyclones. These originate in the Atlantic and track east across the Mediterranean Sea, forming a series of subsynoptic low pressure systems. In winter, outbreaks of cold air plunging south over the relatively warm Mediterranean enhance cyclogenesis, creating the Cyprus Low (Fig. 1). These low pressure systems drive moist air onshore generating intense orographic rainfall across the mountains of the northern Levant. The duration, intensity and track of these storm systems strongly influence the amount of rainfall in this region.

Conditions during the Last Interglacial Period (LIG) are thought to have been similar to that of today. Marine Isotope Stage 5 is generally known as a period of minimum ice volume between 130 to 75 ka (Emiliani, 1955). The Last Interglacial Period (LIG), often defined as being equivalent to MIS 5e (Shackleton et al., 2002), was characterized by a global mean surface temperature at least 2 °C warmer than present (Otto-Bliesner et al., 2006), caused by the orbital forcing of insolation (Berger and Loutre, 1991). The mean sea-level stood 4 to 6 m higher than present (Kopp et al., 2009), with an important contribution from the Greenland ice sheet (Cuffey and Marshall, 2000). The warmest interval, MIS 5e, was followed by two cold episodes in the ocean (MIS 5d and MIS 5b), alternating with two warmer periods (MIS 5c and MIS 5a).

CPD

11, 3241–3275, 2015

Paleoclimate reconstruction in the Levant region

C. Nehme et al.

Title Page

Abstract

Introduction

Conclusions

References

Tables

Figures



Back

Close

Full Screen / Esc

Printer-friendly Version

Interactive Discussion



Paleoclimate reconstruction in the Levant region

C. Nehme et al.

Title Page

Abstract

Introduction

Conclusions

References

Tables

Figures



Back

Close

Full Screen / Esc

Printer-friendly Version

Interactive Discussion



In the eastern Mediterranean basin, periods of anoxic conditions associated with the formation of sapropels during MIS 5 are generally related to wet conditions. These horizons are considered to have formed during periods of increased discharge down the River Nile (Rohling et al., 2002, 2004; Scrivner et al., 2004), linked to enhanced low-latitude hydrological activity in the Nile headwaters. This peak in rainfall corresponds closely with high summer insolation (Rohling et al., 2002; Moller et al., 2012) and with minima in the precession cycle (Lourens et al., 1996). At that time, the East Mediterranean region also experienced enhanced pluvial conditions (Cheddadi and Rossignol-Strick, 1995; Rossignol-Strick and Paterne, 1999; Kallel et al., 2000). Wet conditions are demonstrated by pollen assemblages found within sapropel S5 from the northeastern Mediterranean basin (Cheddadi and Rossignol-Strick, 1995).

Onshore, the climate in the Levant region during MIS 5 has been reconstructed from lacustrine records from interior lake basins such as the Dead Sea and Yammouneh (Kolodny et al., 2005; Gasse et al., 2011, 2015) and speleothem records from central and southern Israel (Frumkin et al., 1999, 2000; Bar-Mathews et al., 1999, 2000; 2003; Ayalon et al., 2013; Vaks et al., 2006, 2013). These archives suggest that climate was generally wet and cold during Termination II (~ 140 – 130 ka). After Termination II, the region experienced an intense warm period coinciding with the development of Sapropel 5 (S5) in the Eastern Mediterranean (Rossignol-Strick and Paterne, 1999; Emeis et al., 2003; Rohling et al., 2002; Ziegler et al., 2010). From ~ 130 – 120 ka, speleothem records from the Peqiin, Soreq and West Jerusalem caves show periods of rapid growth and decrease in $\delta^{18}\text{O}$ values mainly attributed to higher rainfall, suggesting conditions were wetter than during Early Holocene period (Bar-Mathews et al., 2000, 2003). Corresponding high $\delta^{13}\text{C}$ records ($\sim 0\text{‰}$) approaching those of the host carbonate were interpreted as a consequence of soil denudation due to high surface runoff in Soreq cave (Bar-Mathews et al., 2003). However, relatively high ($\sim -5\text{‰}$) and fluctuating $\delta^{13}\text{C}$ in the West Jerusalem cave suggest extremely dry and unstable conditions during which a C4 vegetation type was introduced in this area (Frumkin et al., 2000). Gasse et al. (2011, 2015) suggest wet conditions (~ 125 – 117 ka) as shown in

Paleoclimate reconstruction in the Levant region

C. Nehme et al.

[Title Page](#)

[Abstract](#)

[Introduction](#)

[Conclusions](#)

[References](#)

[Tables](#)

[Figures](#)



[Back](#)

[Close](#)

[Full Screen / Esc](#)

[Printer-friendly Version](#)

[Interactive Discussion](#)



the pollen assemblages and oxygen isotopes from the Yammouneh paleolake, in northern Lebanon. In contrast, the Dead Sea Basin located southwards (Fig. 1), remained dry during this period (Kolodny et al., 2005). The Samra, Amora, and Lisan lakes, precursors of the Dead Sea, showed lower stands than during the Holocene, even though a slight rise occurred during the last Interglacial Maximum (Waldmann et al., 2009).

The return to slightly drier conditions, as suggested by an increase in $\delta^{18}\text{O}$ in speleothems from the Soreq and Peqiin caves is dated at ~ 118 – 120 ka (Bar-Mathews et al., 2000, 2003). Lower rainfall amounts prevailed until 110 ka. But the decrease in $\delta^{13}\text{C}$ in speleothems from these caves (Fig. 1) evidence a reintroduction of a C3 vegetation cover, indicative of wet conditions (Frumkin et al., 2000). In northern Lebanon the Yammouneh paleolake records (Develle et al., 2011) located at higher altitude suggest seasonal changes with wet winters, dry summers and expanded steppe vegetation cover.

From ~ 110 to ~ 100 ka, a moderate wet period is suggested by depleted $\delta^{18}\text{O}$ values in speleothems from Soreq and Peqiin Caves and by an increase in arboreal pollen taxa in northern Lebanon (Develle et al., 2011). This coincides with anoxic conditions (S4) in the eastern Mediterranean (Emeis et al., 2003). Between ~ 100 and ~ 85 ka, a return to a slightly drier climate is suggested by speleothem deposition in both the Soreq and Peqiin caves with an increase in $\delta^{18}\text{O}$ values. However, the continued and more stable C3 vegetation cover (Frumkin et al., 2000) in West Jerusalem cave and the minor lake level increase in the Dead Sea Basin suggest that the climate was probably wetter in the Dead Sea basin (Waldmann et al., 2009). In northern Lebanon, the high altitude Yammouneh paleolake records suggest seasonal variations with steppe vegetation cover similar to the MIS 5d period.

From ~ 85 to ~ 75 ka, the last wet and warm phase of MIS 5 occurred in the Levant, corresponding with Sapropel (S3) in the eastern Mediterranean. In Soreq, Peqiin (Bar-Mathews et al., 1999, 2003) and Ma'aele Efrayim caves (Vaks et al., 2003, 2006), depleted speleothem $\delta^{18}\text{O}$ values suggest a moderate wet period at this time in agreement with the increase in arboreal pollen taxa in the Yammouneh lacustrine record

(Develle et al., 2011). However, the level of Lake Samra in the Dead Sea Basin decreased significantly (Waldmann et al., 2009) and little speleothem deposition occurred in caves situated in the Negev desert (Fig. 1) after MIS 5c (Vaks et al., 2006, 2013), both suggesting a drier climate during MIS 5a in the south of the region.

It is clear that there are significant discrepancies between the climatic records between northern (Lebanon, northern Syria and SE Turkey) and southern Levant (Jordan, Israel/Palestine), possibly driven by a strong north–south palaeoclimatic gradient that varied dramatically in amplitude over short distances and different climatic trends (wet/dry) especially during MIS 5e. In the northern Levant, few records span the MIS 5 period (Gasse et al., 2011, 2015; Develle et al., 2011). New well-dated speleothem records are needed from this area to decipher if and when the climatic changes that are well recorded in the southern Levant (Dead Sea basin, Soreq Cave and Peqiin Caves on the Judean plateau) also affected the northern Levant (Yammouneh, Western Mount-Lebanon). What is still unclear is how the entire region has responded to the North Atlantic/Mediterranean system vs. the southern influences linked to the monsoon system (Arz et al., 2003; Waldmann et al., 2009; Vaks et al., 2013). The K1-2010 speleothem from Kanaan Cave, Lebanon partly fills the disparity in spatial data coverage in the Levant, and may help understand the spatial climate heterogeneity, if any, of the paleoclimatic patterns.

3 Location of Kanaan Cave

Kanaan Cave is located on the western flank of central Mount Lebanon, 15 km north-east of Beirut at 33°54'25" N; 35°36'25" E. The cave has developed in the Middle Jurassic Kesrouane Formation, a thick predominantly micritic limestone and dolomite sequence with an average stratigraphic thickness of 1000 m (Fig. 2a). Being located only 2.5 km from the Mediterranean coast and at just 98 m a.s.l., the cave is strongly influenced by the maritime Mediterranean climate.

Paleoclimate reconstruction in the Levant region

C. Nehme et al.

Title Page

Abstract

Introduction

Conclusions

References

Tables

Figures



Back

Close

Full Screen / Esc

Printer-friendly Version

Interactive Discussion



Paleoclimate reconstruction in the Levant region

C. Nehme et al.

[Title Page](#)

[Abstract](#)

[Introduction](#)

[Conclusions](#)

[References](#)

[Tables](#)

[Figures](#)



[Back](#)

[Close](#)

[Full Screen / Esc](#)

[Printer-friendly Version](#)

[Interactive Discussion](#)



Kanaan Cave is a 162 m long relict conduit discovered during quarrying in 1997. A 23 cm long stalagmite, sample K1-2010 was collected from the top of a fallen limestone block in the center part of the Collapse I chamber, approximately 20 m from the (formerly closed) cave entrance (Fig. 2b and c). The fallen block rests on an unknown thickness of sediment. The passage height at this location is 2.4 m with approximately 50 m of limestone overburden. Presently, the stalagmite receives no dripping water, although some drip water occurs in other parts of the Collapse I chamber during winter and spring seasons. The cave is generally dry during the summer months. The air temperature in Collapse I chamber is $20 \pm 1^\circ\text{C}$.

4 Methods

The stalagmite (sample K1-2010) was cut along its growth axis after retrieval from the cave, and polished using 120–4000 μm silicon carbide (SiC) paper. Petrographic observations were performed with an optical binocular microscope NEOC.

U series dating was carried out at the NERC Isotope Geosciences Laboratory (NIGL), British Geological Survey, Keyworth, UK. Powdered 100 to 400 mg calcite samples were collected with a dental drill from eleven levels along the growth axis of the speleothem, taking care to sample along growth horizons. Chemical separation and purification of uranium and thorium were performed following the procedures of Edwards et al. (1988) with modifications. Data were obtained on a Thermo Neptune Plus multicollector inductively coupled plasma mass spectrometer (MC-ICP-MS) following procedures modified from Anderson et al. (2008) and Hiess et al. (2012). Mass bias and SEM gain for Th measurements were corrected using an in-house ^{229}Th – ^{230}Th – ^{232}Th reference solution calibrated against CRM 112a. Quoted uncertainties for activity ratios, initial $^{234}\text{U}/^{238}\text{U}$, and ages include a ca. 0.2 % uncertainty calculated from the combined $^{236}\text{U}/^{229}\text{Th}$ tracer calibration uncertainty and measurement reproducibility of reference materials (HU-1, CRM 112a, in-house Th reference solution) as well as the measured isotope ratio uncertainty. Ages are calculated from time of analysis (2014)

and also in years before 1950 with an uncertainty at the 2σ level, typically of between 500 and 1000 years (see Table 1).

Samples for $\delta^{13}\text{C}$ and $\delta^{18}\text{O}$ measurements were drilled along the speleothem central axis using a 1 mm dental drill. Ethanol was used to clean the speleothem surface and drill bit prior to sampling. Sample resolution was 1 to 1.2 mm. A total of 206 samples were taken along the longitudinal axis of the stalagmite. Isotopic equilibrium with Hendy tests was carried out (Hendy, 1971) at five different locations along the speleothem axis by drilling samples along an individual growth layer. No evidence for severe out-of-equilibrium deposition was detected along the growth axis of the stalagmite, where the samples for isotope analysis are taken.

Three seepage water samples and three water pool samples from Kanaan Cave were collected for $\delta^{18}\text{O}$ measurements in hermetically sealed glass bottles. Measurements were performed at the Vrije Universiteit Brussel on a Picarro L2130-i analyzer using the cavity-ring down spectroscopy (CRDS) technique. All values are reported in per mill (‰) relative to Vienna Standard Mean Ocean Water (V-SMOW2). Analytical uncertainties (2σ) were less than 0.10 ‰.

5 Results

5.1 Petrography

The speleothem collected from Kanaan Cave is 23 cm long and up to 10 cm wide (Fig. 2). In section it displays regular layers of dense calcite ranging in colour from dark brown to light yellow with a regular thin (< 0.2 mm) lamination in places. The speleothem has two clearly defined growth phases, characterized by an abrupt hiatus where the stalagmite was tilted around 45° and then recommenced growing.

The lower segment (Segment 1) is 8.2 cm long and 8.5 cm wide (Fig. 3) and displays a general growth axis tilted at a 45° angle (clockwise) relative to upper segment. The regular deposition of translucent columnar crystals is interrupted by clayey lay-

CPD

11, 3241–3275, 2015

Paleoclimate reconstruction in the Levant region

C. Nehme et al.

Title Page

Abstract

Introduction

Conclusions

References

Tables

Figures



Back

Close

Full Screen / Esc

Printer-friendly Version

Interactive Discussion



ers (discontinuities) mostly at 17 cm, from 15.6 to 15.2 cm and at 14.2 cm. Between 12.2 and 14.2 cm, the lamina in the central axial part of the speleothem show continuous clear and translucent layering, but which becomes increasingly clayey towards the outer edge of the sample. The higher segment (Segment 2) is 12.3 cm long and 4–6 cm wide. At the base, the general growth axis is tilted at 16° (counter clockwise) to the azimuth axis, gradually becoming more vertical towards the top. The general structure of this section is characterized by uniform yellow translucent columnar crystals interrupted by marked opaque yellow layers, respectively at 9, 8, 5.6, 3.2 and 2.8 cm.

5.2 Uranium series (U–Th) dating

Ten uranium series dates, shown in Table 1 indicate that the stalagmite K1-2010 grew from approximately 129.72 ± 0.8 (2σ) to 85.3 ± 0.7 ka. An extrapolated age of 84.1 ka for the top of the stalagmite was calculated from the age model in Fig. 4 obtained by plotting an age vs. depth profile on grapher. StalAge program was not suitable for obtaining an automated age model due to discontinuities on the stalagmite growth profile. The measured uncertainties are highest in the lower part of the speleothem where detrital layers prevail. The dates are in stratigraphical order with the exception of sample KA-stm-6. Several discontinuities were noted in the middle and towards the base, leading to uncertainties in determining a basal age for the speleothem. A basal age of ~ 132.1 ka was estimated by extrapolating the speleothem age model downwards using the growth rate between 124.5 ± 1.1 and 126.0 ± 0.8 ka. The major discontinuity in the middle part of the speleothem as shown in Fig. 4 lasted from 108.8 (intrapolated) to 103.5 ka (intrapolated) during which the growth axis was tilted by about 45° .

5.3 Modern cave water and calcite isotopic compositions

Recent cave water (a proxy for rainfall $\delta^{18}\text{O}$) sampled from the cave shows an average $\delta^{18}\text{O}$ value of $-5.43 \pm 0.06\text{‰}$. $\delta^{18}\text{O}$ and δD seepage water values in Kanaan Cave falls on the local meteoric waterline (Saad et al., 2005) indicating that no severe evaporation

Title Page

Abstract

Introduction

Conclusions

References

Tables

Figures



Back

Close

Full Screen / Esc

Printer-friendly Version

Interactive Discussion



processes occur in the epikarst before precipitating the speleothem. Using the Kim and O'Neil (1997) equilibrium equation, calcite precipitated under these conditions should theoretically display $\delta^{18}\text{O}$ values around ca. -4.6‰ $(20\text{ °C})^{-1}$, the present temperature in the cave.

5.4 Oxygen and Carbon isotope series

If precipitation occurs at isotopic equilibrium, the calcite $\delta^{18}\text{O}$ should not show any significant enrichment along a single lamina away from the growth axis and no covariation between $\delta^{18}\text{O}$ and $\delta^{13}\text{C}$ should occur. As indicated by several of these so-called Hendy tests (Hendy, 1971) performed along growth layers, no severe out-of-equilibrium processes during precipitation of the calcite seem to have occurred (see Supplement).

The $\delta^{18}\text{O}$ values from K1-2010 (Fig. 5) ranged from -3.5 to -7.8‰ , with an overall mean of -5.1‰ . Lower values ($\sim -7.5\text{‰}$) are observed at the basal part of the stalagmite. Values increase rapidly to $\sim -4.5\text{‰}$ at 122.7 ka. High $\delta^{18}\text{O}$ values (generally between -4.7 and -4‰) are observed until the top of the stalagmite at ~ 84 ka, except for two periods with relatively lower $\delta^{18}\text{O}$. From 103.4 to 100.2 ka, the $\delta^{18}\text{O}$ values decrease from -4.6 to -6.18‰ in ~ 1.5 ka. At 94 ka, a rapid decrease of $\delta^{18}\text{O}$ values leads to a peak of -5.5‰ at 92.7 ka. The top of the stalagmite at ~ 84 ka exhibit the highest $\delta^{18}\text{O}$ values of -3.5‰ . The $\delta^{13}\text{C}$ V-PDB values range between -10.0 and -12.4‰ with an overall mean of -11.3‰ as shown in Fig. 5. The $\delta^{13}\text{C}$ curve shows relatively minor variations. However, the most depleted values (-12‰) are observed at the base of the speleothem, before 130 ka, followed by a minor $\delta^{13}\text{C}$ enrichment of $\sim 1\text{‰}$ from 124 to 120 ka and stays around -11‰ between 120 and 110 ka. After 110 ka generally lower $\delta^{13}\text{C}$ values prevail with a surprising stable period between ~ 100 and 93 ka. From ~ 93 to 90 ka, a 1.1‰ enrichment of carbon isotopic values leads to highest $\delta^{13}\text{C}$ values of the time series. Consequently, the stalagmite shows a tripartite partition as shown in the $\delta^{18}\text{O}$ V-PDB vs. $\delta^{13}\text{C}$ V-PDB diagram (Fig. 6) with the base featuring the most depleted $\delta^{18}\text{O}$ and $\delta^{13}\text{C}$ values before 129 ka. A rapid shift towards higher isotopic values between ~ 125.4 and ~ 122 ka and a third segment, from

Paleoclimate reconstruction in the Levant region

C. Nehme et al.

Title Page

Abstract

Introduction

Conclusions

References

Tables

Figures



Back

Close

Full Screen / Esc

Printer-friendly Version

Interactive Discussion



~ 122 to ~ 84 ka, shows rather stable $\delta^{13}\text{C}$ and $\delta^{18}\text{O}$ values except for the 103–101 and 93–90 ka characterized by a change to lower isotopic values for oxygen and higher values for carbon.

6 Discussion

6.1 Integrated climatic interpretation of the speleothem proxies

Speleothem growth is conditioned by effective precipitation and CO_2 concentration, controlled mainly by the bio-activity of the soil and consequently by the temperature (Baker and Smart, 1995; Dreybrodt, 1988; Genty et al., 2006). Therefore speleothem growth is typically associated with warm and humid conditions with sufficient rainfall to maintain drip-water flow, whereas low speleothem growth rates or hiatuses tend to indicate cold or dry conditions (Bar-Matthews et al., 2003), or possibly flooding. Two hiatuses are identified in the K1-2010 stalagmite. The first hiatus occurs between ~ 129.5 and ~ 126 ka, after a period of growth associated with the start of the Last Interglacial Period. The speleothem stops growing shortly after the onset of MIS 5e (Shackleton et al., 2002). Given the expectation that MIS5e would be warm and wet, the cessation of growth at this time is unexpected. However, the lower part of the stalagmite deposited at this time contains several clayey layers that may indicate either long dry periods, or periods during which the speleothem was covered with mud or muddy water. The fact that apart from these muddy layers the speleothem does not show any change in crystal aspect or change in porosity, suggests that these hiatuses may be better explained by sudden events perturbing speleothem deposition rather than a significant increase in aridity or drop in temperature leading to cessation of growth. The stalagmite was collected from a rock situated in the center of a small depression in the cave floor. It is plausible that a small muddy pool may have been formed in the depression and may have covered the fallen block and speleothem growing on it. This scenario would explain the sudden cessation of speleothem deposition after the initial onset of growth

**Paleoclimate
reconstruction in the
Levant region**

C. Nehme et al.

[Title Page](#)[Abstract](#)[Introduction](#)[Conclusions](#)[References](#)[Tables](#)[Figures](#)[Back](#)[Close](#)[Full Screen / Esc](#)[Printer-friendly Version](#)[Interactive Discussion](#)

during the humid conditions in first part of the LIG. Previous studies in Southern Europe (Drysdale et al., 2005; Zanchetta et al., 2007) and in the Eastern Levant (Bar-Mathews et al., 2003; Frumkin et al., 2000; Verheyden et al., 2008) have shown that most of the carbon in speleothem calcite is derived from soil CO₂ (Genty et al., 2001). The $\delta^{13}\text{C}$ is thus most likely to be controlled by biogenic soil CO₂ productivity (Gascoyne, 1992; Hellstrom et al., 1998; Genty et al., 2006) associated with vegetation density, which regulates soil CO₂ content via root respiration, photosynthetic and microbial activity. The changes in carbon isotopic composition ($\delta^{13}\text{C}$) of speleothems in the Levant are thus linked to changes in precipitation with periods of low rainfall inducing sparse vegetation and a lower contribution of “light” organic carbon in the speleothem resulting in higher $\delta^{13}\text{C}$ value (Frumkin et al., 2000). The low values for $\delta^{13}\text{C}$ in the K1-2010 around ~ 129 ka are indicative of a 100 % C3 vegetation profile with relatively high soil productivity suggestive of rather mild and humid conditions.

Other discontinuities are observed in the first segment of the speleothem but do not seem to be related to long hiatuses, with the fact that the high growth rate is observed in the middle part of segment 1. A second hiatus was estimated to occur between ~ 109 and ~ 103 ka by extrapolating the growth rates of each segment towards the discontinuity D2. This discontinuity, marked by a relatively thick clay layer, is associated with a major change in speleothem orientation. During this hiatus, the stalagmite was tilted by around 45° , most probably due to sediment washing out and causing the block on which the stalagmite grew to move. A striking decrease in the growth rate to $0.013\text{ cm (100 yr)}^{-1}$ before the speleothem tilted seems to start at ~ 119 ka, corresponding to the onset of the last glacial. Additional U-series dates are necessary to better constrain the age of the change in growth rate.

The middle part shows a higher growth rate ($0.09\text{ cm (100 yr)}^{-1}$) from ~ 103 to ~ 99.8 ka during the ensuing interstadial (MIS 5c), followed by a decrease in both growth rate (0.03 to $0.06\text{ cm (100 yr)}^{-1}$) and speleothem diameter from ~ 99.8 to ~ 85.3 ka during MIS 5b. The carbon isotope signal shifts slightly to more positive val-

ues around ~ 124 – 121 ka and has the most positive values after ~ 92 ka, indicating a gradual degradation of the soil coverage at the beginning of MIS 5d.

Unraveling the factors controlling the $\delta^{18}\text{O}$ signal in a speleothem can be more complex (McDermott, 2004; Fairchild et al., 2006; Lachniet, 2009). The pattern of $\delta^{18}\text{O}$ changes in K1-2010 stalagmite are slightly different from the $\delta^{13}\text{C}$, particularly the difference in the amplitude of changes between ~ 124 and 120 ka, and from 120 to 84 ka.

Speleothem $\delta^{18}\text{O}$ is controlled by both the calcite precipitation temperature (Kim and O'Neil, 1997) and seepage water $\delta^{18}\text{O}$ (Lachniet, 2009). The general consensus in recent years is that the principal driver of speleothem $\delta^{18}\text{O}$ variations through time is change in rainfall $\delta^{18}\text{O}$ (McDermott, 2004), which are forced by: (i) condensation temperatures, (ii) rainfall amount (Dansgaard, 1964), (iii) shifts in vapor source $\delta^{18}\text{O}$ or, (iv) different air–mass trajectories (Rozanski et al., 1993). Until now, low speleothem $\delta^{18}\text{O}$ values in the Levant region were associated with wetter conditions while high speleothem $\delta^{18}\text{O}$ was generally ascribed to drier periods with lower rainfall amounts (Bar-Mathews, 2014; Verheyden et al., 2008). Important changes in $\delta^{18}\text{O}$ may however also been linked to changes in the source of the water vapor and/or changes in storm-tracks (Frumkin et al., 1999; Kolodny et al., 2005; McGarry et al., 2004). From ~ 125 to ~ 124 ka, the abrupt 2.8‰ increase in $\delta^{18}\text{O}$ values suggests an important change to drier conditions. The growth rate of the stalagmite gradually falls from a high rate between 126.0 ± 0.8 and 124.5 ± 1.1 ka, decreasing to $0.03 \text{ mm } (100 \text{ a})^{-1}$ between 124.5 ± 1.1 and 119.84 ± 1.5 ka, and to $0.013 \text{ mm } (100 \text{ a})^{-1}$ after ~ 120 ka. This gradual drop in growth rate most probably indicates a change towards drier conditions in agreement with the increase in $\delta^{18}\text{O}$ values. Global sea-levels reached 6 to 9 m above present sea-level during the LIG (Dutton and Lambeck, 2012), an elevation peak that could not be responsible for the observed $\delta^{18}\text{O}$ change. Another mechanism is a change in the composition and source of water vapor reaching the site. Studies of the Eastern (EM), Central and Western Mediterranean marine core records show evidence of reduced sea-surface $\delta^{18}\text{O}$ during the onset of the Sapropel 5 event of $\sim 2\text{‰}$ (e.g. Kallel et al., 1997, 2000; Emeis et al., 2003; Rohling et al., 2002; Scrivner et al.,

Paleoclimate reconstruction in the Levant region

C. Nehme et al.

[Title Page](#)[Abstract](#)[Introduction](#)[Conclusions](#)[References](#)[Tables](#)[Figures](#)[Back](#)[Close](#)[Full Screen / Esc](#)[Printer-friendly Version](#)[Interactive Discussion](#)

**Paleoclimate
reconstruction in the
Levant region**

C. Nehme et al.

[Title Page](#)[Abstract](#)[Introduction](#)[Conclusions](#)[References](#)[Tables](#)[Figures](#)[Back](#)[Close](#)[Full Screen / Esc](#)[Printer-friendly Version](#)[Interactive Discussion](#)

2004; Ziegler et al., 2010; Grant et al., 2012) and a recovery of the same amount at the end of S5 deposition around ~ 121 ka (Grant et al., 2012), with a commensurate increase in the $\delta^{18}\text{O}$ of the EM water. Hence, a more ^{18}O -enriched sea surface of $\sim 2\%$ at the end of the sapropel event would cause an increase in vapor $\delta^{18}\text{O}$, leading to enrichment in the isotopic composition of the recharge waters reaching the cave. In the Levant, moisture source was interpreted as one of the drivers for the $\delta^{18}\text{O}$ signal in speleothems from Soreq Cave (Bar-Mathews et al., 2003) related to sapropel S5 (128–121 ka; Grant et al., 2012).

After ~ 122 ka, the $\delta^{18}\text{O}$ increased to an average of $\sim -4.3\%$, suggesting less depleted precipitation was reaching the cave until ~ 84 ka. This long-term $\delta^{18}\text{O}$ enrichment, interrupted by a short and moderate $\delta^{18}\text{O}$ decrease during sapropel S4, marks the onset of a Northern Hemisphere glaciation. This increase in $\delta^{18}\text{O}$ is driven by several mechanisms. Once cause, the “ice volume effect” can lead to a higher sea water $\delta^{18}\text{O}$ by 1.1‰ during glacial periods together with an increase in $\delta^{18}\text{O}$ due to drop in temperature of up to $\sim 8^\circ\text{C}$ (Frumkin et al., 1999; Bar-Mathews et al., 2003; Kolodny et al., 2005; McGarry et al., 2004). However, the abrupt change in the K1 speleothem is not in agreement with the gradual change of the global IG-G changes suggesting a stronger influence of other mechanisms. A second possible driver for increased $\delta^{18}\text{O}$ is related to changes in wind direction, with more continental trajectories leading to more enriched $\delta^{18}\text{O}$ water vapor reaching the cave. In Southern Levant, Frumkin et al. (1999) and Kolodny et al. (2005) related $\delta^{18}\text{O}$ signal increase during glacial periods to a southward migration of the Westerlies associated with the high-pressure zone over the Northern European ice sheet and thus pushing wind trajectories further south over North Africa. The growth rate of the stalagmite after ~ 120 ka is the lowest of the entire profile (between 0.013 and $0.06\text{ mm}(100\text{ a})^{-1}$) except for the period between 102.5 ± 0.9 and 99.87 ± 0.7 ka which has a moderate growth rate of $0.09\text{ mm}(100\text{ a})^{-1}$. This wet pulse coincides with the S4 event. The discontinuity D2, between ~ 108.8 and ~ 103.5 ka is probably linked to increased rainfall during this pe-

riod. Increased drip-water flux through the cave flushed out the sediment floor beneath the stalagmite block, causing the speleothem to subside and tilt.

6.2 Paleoclimate variability of MIS 5

6.2.1 An “early humid LIG”

Speleothem oxygen, carbon and growth proxies from sample K1-2010 indicate an initial relatively warm and humid period at ~ 129 ka – the beginning of the LIG – which extended until ~ 125.4 ka. The lack of any speleothem growth from ~ 129 – 126 ka (discontinuity D1) is most probably related to extreme wet conditions leading to the formation of a local pool in the cave, submerging the stalagmite. This early humid LIG matches the timing of Eastern Mediterranean Sea Sapropel 5 event (Ziegler et al., 2010; Grant et al., 2012) with high summer insolation (Berger and Loutre, 1991). In southern Europe, an early commencement of full interglacial conditions was dated at 129 ± 1 ka in Corchia Cave speleothems (Drysdale et al., 2005). In northern Levant, the pollen records in Yammouneh paleolake demonstrate the presence of temperate oaks during the early LIG (Develle et al., 2011) indicating sufficient humidity to enable forests to develop. More efficient moisture retention together with developed forest landscapes and intense groundwater circulation in northern Lebanon prevailed during the LIG. These warm and wet conditions are in agreement with similar periods identified in the Lake Van lacustrine sequence (Litt et al., 2014; Stockhecke et al., 2014) in North-Eastern Turkey and with speleothem proxies from Soreq and Peqiin caves (Ayalon et al., 2002; Bar-Mathews et al., 2003) in southwestern Israel.

6.2.2 The 125 ka change

The pattern of $\delta^{18}\text{O}$ depletion from sample K1-2010 records a remarkable change between ~ 125.4 to ~ 122 ka along with an unstable depletion pattern of the $\delta^{13}\text{C}$ and the $\delta^{18}\text{O}$. However, the poor chronological resolution of this part of the K1-2010

Paleoclimate reconstruction in the Levant region

C. Nehme et al.

Title Page

Abstract

Introduction

Conclusions

References

Tables

Figures



Back

Close

Full Screen / Esc

Printer-friendly Version

Interactive Discussion



speleothem record precludes the identification of any seasonality pattern at the end of the LIG, as seen in the Yammouneh lacustrine record in northern Lebanon (Develle et al., 2011; Gasse et al., 2015).

The K1-2010 $\delta^{18}\text{O}$ profile undergoes a dramatic change around ~ 125.4 ka, the timing of which is very close to the onset of the isotopic enrichment of the water source in the eastern Mediterranean Sea during the S5 event (~ 128 – 121 ka). The time phasing is calculated for a 1000 years time lag between the K1-2010 isotopic change (~ 125.4 ka) and the $\delta^{18}\text{O}_{\text{g.ruber}}$ enrichment onset in LC21 core (Grant et al., 2012) and in ODP 967 site (Emeis et al., 2003). The time lag is reduced to only 500 years compared to the $\delta^{18}\text{O}$ profile in MD-74 core (Emeis et al., 2003). Despite differences in dating resolution between marine core records and speleothems, the shift in K1-2010 $\delta^{18}\text{O}$ values around ~ 125.4 ka demonstrates a major source-driven change during the eastern Mediterranean S5 event. Several studies (Rohling et al., 2002, 2004; Schmiiedl et al., 2003; Scrivner et al., 2004) suggest a coincidence between cooling and enhanced aridity around the Mediterranean, and the interruption of the insolation-driven monsoon maximum for a millennial-scale episode during the last interglacial sapropel S5. Schmiiedl et al. (2003) argue that this episode marked the onset of a regional climate deterioration following the peak (early S5) of the last interglacial. In that case, this regional climate deterioration began at ~ 126 ka, using the S5 timing of Grant et al. (2012) and with the assumed linear sedimentation rate through S5 (Rohling et al., 2002b). The K1-2010 isotopic profile confirms this and provides a precise chronology of the change, taking place between 126.0 ± 0.8 and 122 ka (interpolated).

The K1-2010 $\delta^{18}\text{O}$ profile indicates this major change occurred earlier than other continental records in the Levant region suggest. The timing of the change in K1-2010 $\delta^{18}\text{O}$ and $\delta^{13}\text{C}$ profiles lasted 4000 years along with a gradual pattern and stops at 122 ka (interpolated). A similar gradual variation but over a larger time scale was demonstrated in the Yammouneh paleovegetation signal, where the transition seems to be more progressive than in other Eastern Mediterranean records. In Southern Levant, the oxygen and carbon isotopic record in Peqiin and Soreq cave suggest an abrupt

Paleoclimate reconstruction in the Levant region

C. Nehme et al.

Title Page

Abstract

Introduction

Conclusions

References

Tables

Figures



Back

Close

Full Screen / Esc

Printer-friendly Version

Interactive Discussion



but later enrichment signal around ~ 118 ka (Bar-Mathews et al., 2003). This change was shifted to ~ 122 ka (Grant et al., 2012) using a more refined U–Th chronology.

6.2.3 The glacial inception

After ~ 122 ka, a more enriched $\delta^{18}\text{O}$ profile indicates the end of warm and wet conditions of the LIG. The onset of glacial conditions as indicated in several continental records in the Eastern Mediterranean shows a gradual climate deterioration into the full glacial conditions of MIS 4. The isotopic response of K1-2010 to the glacial inception is recorded synchronously at ~ 122 ka in both $\delta^{18}\text{O}$ and $\delta^{13}\text{C}$ signals, but while the $\delta^{18}\text{O}$ decreases rapidly along with a shift to a moderate growth rate, especially in response to the wet pulses during the S4 event, the $\delta^{13}\text{C}$ shows a more gradual evolution. This is probably explained by the fact that a rainfall- and mostly source-driven $\delta^{18}\text{O}$ signal is rapidly transmitted to K1-2010 speleothem, whereas the inertia and gradual change of the $\delta^{13}\text{C}$ signal reflect the time required for the soil and biopedological activity above the cave to respond on a long-term scale. On a regional scale, the Yammouneh paleovegetation signal indicates expanded steppic vegetation cover after ~ 120 ka (Develle et al., 2011). In southern Levant, a gradual $\delta^{13}\text{C}$ and $\delta^{18}\text{O}$ enrichment, except for the wet pulses during the S4 and S3 events, until the end of the MIS 5 indicate a general climate degradation that could be related to less rainfall derived from the Mediterranean moisture source (Ayalon et al., 2002; Bar-Mathews et al., 2003) or to changes in wind circulation pattern (Kolodny et al., 2005; Lisker et al., 2010). Further south in the Negev region, a different climatic regime from the Northern Levant is recorded from speleothems and lacustrine records. Speleothem growth rates decreased after MIS 5c (Vaks et al., 2006, 2013), with less rainfall from the Mediterranean sea reaching the Negev, while the Mudawwara paleolake in southern Jordan showed a wet pulse during the MIS 5a, related more to rainfall originating from the Indian monsoon (Petit-Maire et al., 2010). Moreover, Lake Samra records in the Dead Sea basin are not in phase with Levantine records further north and show low lake-levels during MIS 5c and 5a and minor high levels during MIS 5d and 5b (Waldmann

Paleoclimate reconstruction in the Levant region

C. Nehme et al.

Title Page

Abstract

Introduction

Conclusions

References

Tables

Figures



Back

Close

Full Screen / Esc

Printer-friendly Version

Interactive Discussion



et al., 2009). The climate picture of the Dead Sea basin during the glacial inception is related probably to local factors influenced by the Judean rain shadow (Vaks et al., 2006, 2013) and together with other continental records further south, invoke climatic variations driven by the monsoon system and its boundary shifts (Parton et al., 2015; 5 Bar-Mathews et al., 2014).

7 Conclusions

A dated MIS 5 stalagmite record (129–84 ka) from Kanaan Cave, Lebanon demonstrates the potential of stalagmite records for palaeoclimate reconstruction in the northern Levant. The K1-2010 model age coupled with growth rates and isotopic data provide a more precise record of the climatic changes that occurred during the last interglacial and on into the glacial inception period. 10

The K1-2010 speleothem record indicate a very wet early LIG and during the LIG optimum at the global scale, and is in agreement with warm and humid conditions demonstrated in other speleothem and lacustrine records from the Mediterranean. 15 The K1-2010 isotope record and growth rate curves clearly demonstrate an important change from 126.0 ± 0.8 to 122 ka (intrapolated). The change seems to be driven by a “source” effect, reflecting the $\delta^{18}\text{O}$ Mediterranean Sea surface water composition and remarkably follows, both in time and amplitude, the EM isotopic increase at ~ 126 ka during the S5 event. This change sets the onset of the regional climate deterioration following the peak (early S5) of the last interglacial over the Levant region. However, 20 the climatic change as recorded in the K1-2010 isotopic record is more gradual than the changes identified in the Soreq and Peqiin speleothem records.

After ~ 122 ka, enriched oxygen and carbon profiles in K1-2010 document the end of the early LIG humid phase. The change in isotopic composition is driven by a reduction in rainfall originating from the Mediterranean Sea, coupled with a long-term 25 change in the $\delta^{18}\text{O}$ composition of the EM surface waters. The onset of glacial conditions, as indicated in several continental records in the Levant, is signified by a gradual

climatic deterioration until the full glacial conditions of the MIS 4. A short, wet phase (~ 103–100 ka) at the end of the S4 event is indicated by increased water ingress into Kanaan Cave causing faster speleothem growth rates, sediment flushing, subsidence and speleothem tilting. The climatic scheme suggested from K1-2010 isotopic profiles and growth rates is in overall agreement with Yammouneh paleolake records in northern Lebanon, and with the Soreq and Peqiin speleothems records. However, the K1-2010 record contrasts with the Lake Samra records in the Dead Sea basin, which is driven by local topographic factors together with different hydrologic (local) or climatic (regional) system.

The Supplement related to this article is available online at doi:10.5194/cpd-11-3241-2015-supplement.

Acknowledgements. This study was funded by the mobility fellowship program of the Belgian Federal Scientific Policy (BELSPO), co-funded by the Marie Curie Actions of the European Commission. We acknowledge EDYTEM Laboratory (UMR-5204 CNRS) and Saint-Joseph University for making stalagmites of Kanaan Cave available for analyses during this study. We would like to thank the support of ALES (Association Libanaise d'Études Spéléologiques) members who accompanied us during field trips. Farrant and Noble publish with the approval of the Executive Director, British Geological Survey. We thank Daniel Condon and Diana Sahy for assisting with the uranium series analyses and Kevin De Bont for assisting in water analyses. We also thank the anonymous reviewers for their constructive comments and reviews.

References

- Andersen, M. B., Stirling, C. H., Potter, E. K., Halliday, A. N., Blake, S. G., McCulloch, M. T., Ayling, B. F., and O'Leary, M.: High-precision U-series measurements of more than 500 000 year old fossil corals, *Earth Planet. Sc. Lett.*, 265, 229–245, 2008.
- Arz, H. W., Lamy, F., Patzold, J., Muller, P. J., and Prins, M.: Mediterranean moisture source for an early-Holocene humid period in the northern Red Sea, *Science*, 300, 118–121, 2003.

Paleoclimate reconstruction in the Levant region

C. Nehme et al.

[Title Page](#)

[Abstract](#)

[Introduction](#)

[Conclusions](#)

[References](#)

[Tables](#)

[Figures](#)



[Back](#)

[Close](#)

[Full Screen / Esc](#)

[Printer-friendly Version](#)

[Interactive Discussion](#)



Ayalon, A., Bar-Matthews, M., and Kaufman, A.: Climatic conditions during marine isotopic stage 6 in the Eastern Mediterranean region as evident from the isotopic composition of speleothems: Soreq Cave, Israel, *Geology*, 30, 303–306, 2002.

Ayalon, A., Bar-Matthews, M., Frumkin, A., and Matthews, A.: Last Glacial warm events on Mount Hermon: the southern extension of the Alpine karst range in the east Mediterranean, *Quaternary Sci. Rev.*, 59, 43–56, 2013.

Baker, A. and Smart, P. L.: Recent flowstone growth rates: field measurements in comparison to theoretical predictions, *Chem. Geol.*, 122, 121–128, 1995.

Bar-Matthews, M.: History of Water in the Middle East and North Africa, Elsevier, Amsterdam, 109–128, 2014.

Bar-Matthews, M., Ayalon, A., Kaufman, A., and Wasserburg, G. J.: The Eastern Mediterranean paleoclimate as a reflection of regional events: Soreq Cave, Israel, *Earth Planet. Sc. Lett.*, 166, 85–95, 1999.

Bar-Matthews, M., Ayalon, A., and Kaufman, A.: Timing and hydrological conditions of Saproel events in the Eastern Mediterranean, as evident from speleothems, Soreq Cave, Israel, *Chem. Geol.*, 169, 145–156, 2000.

Bar-Matthews, M., Ayalon, A., Gilmour, M., Matthews, M., and Hawkesworth, C.: Sea–land isotopic relationships from planktonic foraminifera and speleothems in the Eastern Mediterranean region and their implications for paleorainfall during interglacial interval, *Geochim. Cosmochim. Ac.*, 67, 3181–3199, 2003.

Berger, A. and Loutre, M. F.: Insolation values for the climate of the last 10 million years, *Quaternary Sci. Rev.*, 10, 297–317, 1991.

Cheddadi, R. and Rossignol-Strick, M.: Eastern Mediterranean Quaternary paleoclimates from pollen and isotope records of marine cores in the Nile cone area, *Paleoceanography*, 10, 291–300, 1995.

Cheng, H., Edwards, R. L., Broecker, W. S., Denton, G. H., Kong, X., Wang, Y., Zhang, R., and Wang, X.: Ice age terminations, *Science*, 326, 248–252, 2009.

Cuffey, K. M. and Marshall, S. J.: Substantial contribution to sea-level rise during the last interglacial from the Greenland ice sheet, *Nature*, 404, 591–594, 2000.

Develle, A. L., Gasse, F., Vidal, L., Williamson, D., Demory, F., Van Campo, E., Ghaleb, B., and Thouveny, N.: A 250 ka sedimentary record from a small karstic lake in the Northern Levant (Yammoûneh, Lebanon): paleoclimatic implications, *Palaeogeogr. Palaeoclimatol.*, 305, 10–27, 2011.

**Paleoclimate
reconstruction in the
Levant region**

C. Nehme et al.

[Title Page](#)[Abstract](#)[Introduction](#)[Conclusions](#)[References](#)[Tables](#)[Figures](#)[Back](#)[Close](#)[Full Screen / Esc](#)[Printer-friendly Version](#)[Interactive Discussion](#)

Drysdale, R., Zanchetta, G., Hellstrom, J., Fallick, A., and Zhao, J.-X.: Stalagmite evidence for the onset of the Last Interglacial in southern Europe at 129 ± 1 ka, *Geophys. Res. Lett.*, 32, L24708, doi:10.1029/2005GL024658, 2005.

Drysdale, R. N., Zanchetta, G., Hellstrom, J. C., Fallick, A. E., McDonald, J., and Cartwright, I.: Stalagmite evidence for the precise timing of North Atlantic cold events during the early last glacial, *Geology*, 35, 77–80, 2007.

Drysdale, R., Hellstrom, J., Zanchetta, G., Fallick, A. E., Sánchez Goñi, M. F., Couchoud, I., McDonald, J., Maas, R., Lohmann, G., and Isola, I.: Evidence for obliquity forcing of glacial Termination II, *Science*, 325, 1527–1531, 2009.

Dutton, A. and Lambeck, K.: Ice volume and sea level during the last interglacial, *Science*, 337, 216–219, 2012.

Edwards, R. L., Chen, J. H., Ku, T. L., and Wasserburg, G. J.: Precise timing of the last interglacial period from mass-spectrometric determination of ^{230}Th in corals, *Science*, 236, 1547–1553, 1987.

Emeis, K. C., Schulz, H., Struck, U., Rossignol-Strick, M., Erlenkeuser, H., Howell, M. W., Kroon, D., Mackensen, A., Ishizuka, S., Oba, T., Sakamoto, T., and Koizumi, I.: Eastern Mediterranean surface water temperatures and $\delta^{18}\text{O}$ during deposition of sapropels in the late Quaternary, *Paleoceanography*, 18, 1005, doi:10.1029/2000PA000617, 2003.

Emiliani, C.: Pleistocene temperatures, *J. Geol.*, 63, 538–578, 1955.

Enzel, Y., Amit, R., Dayan, U., Crouvi, O., Kahana, R., Ziv, B., and Sharon, D.: The climatic and physiographic controls of the eastern Mediterranean over the late Pleistocene climates in the southern Levant and its neighboring deserts, *Global Planet. Change*, 60, 165–192, 2008.

Fairchild, I. J., Smith, C. L., Baker, A., Fuller, L., Spötl, C., Matthey, D., and McDermott, F.: Modification and preservation of environmental signals in speleothems, *Earth-Sci. Rev.*, 75, 105–153, 2006.

Frumkin, A., Ford, D. C., and Schwarcz, H. P.: Continental oxygen isotopic record of the last 170,000 years in Jerusalem, *Quaternary Res.*, 51, 317–327, 1999.

Frumkin, A., Ford, D. C., and Schwarcz, H.: Paleoclimate and vegetation of the Last Glacial cycles in Jerusalem from a speleothem record, *Global Biogeochem. Cy.*, 14, 863–870, 2000.

Gascoyne, M.: Palaeoclimate determination from cave calcite deposits, *Quaternary Sci. Rev.*, 11, 609–632, 1992.

Paleoclimate reconstruction in the Levant region

C. Nehme et al.

[Title Page](#)[Abstract](#)[Introduction](#)[Conclusions](#)[References](#)[Tables](#)[Figures](#)[Back](#)[Close](#)[Full Screen / Esc](#)[Printer-friendly Version](#)[Interactive Discussion](#)

Gasse, F., Vidal, L., Develle, A.-L., and Van Campo, E.: Hydrological variability in the Northern Levant: a 250 ka multi-proxy record from the Yammoûneh (Lebanon) sedimentary sequence, *Clim. Past*, 7, 1261–1284, doi:10.5194/cp-7-1261-2011, 2011.

Gasse, F., Vidal, L., Van Campo, E., Demory, F., Develle, A.-L., Tachikawa, K., Elias, A., Bard, E., Garcia, M., Sonzogni, C., and Thouveny, N.: Hydroclimatic changes in northern Levant over the past 400 000 years, *Quaternary Sci. Rev.*, 111, 1–8, 2015.

Genty, D., Baker, A., and Vokal, B.: Intra- and inter-annual growth rate of modern stalagmites, *Chem. Geol.*, 176, 191–212, 2001.

Genty, D., Blamart, D., Ouahdi, R., Gilmour, M., Baker, A., Jouzel, J., and Van-Exter, S.: Precise dating of Dansgaard-Oeschger climate oscillations in western Europe from stalagmite data, *Nature*, 421, 833–837, 2003.

Genty, D., Blamart, D., Ghaleb, B., Plagnes, V., Causse, C. H., Bakalowicz, M., Zouari, K., Chkir, N., Hellstrom, J., Wainer, K., and Bourges, F.: Timing and dynamics of the last deglaciation from European and North African $\delta^{13}\text{C}$ stalagmite profiles – comparison with Chinese and South Hemisphere stalagmites, *Quaternary Sci. Rev.*, 25, 2118–2142, 2006.

Grant, K. M., Rohling, E. J., Bar-Matthews, M., Ayalon, A., Medina-Elizalde, M., Bronk Ramsey, C., Satow, C., and Roberts, A. P.: Rapid coupling between ice volume and polar temperature over the past 150 kyr, *Nature* 491, 744–747, 2012.

Hellstrom, J., McCulloch, M., and Stone, J.: A detailed 31 000-year record of climate and vegetation change, from the isotope geochemistry of two New Zealand speleothems, *Quaternary Res.*, 50, 167–178, 1998.

Hendy, C. H.: The isotopic geochemistry of speleothems – I. The calculation of the effects of different modes of formation on the isotopic composition of speleothems and their applicability as palaeoclimatic indicators, *Geochim. Cosmochim. Ac.*, 35, 801–824, 1971.

Hiess, J., Condon, D. J., McLean, N., and Noble, S. R.: $^{238}\text{U}/^{235}\text{U}$ systematics in terrestrial uranium-bearing minerals, *Science*, 335, 1610–1614, 2012.

Kallel, N., Duplessy, J.-C., Labeyrie, L., Fontugne, M., Paterne, M., and Montacer, M.: Mediterranean pluvial periods and sapropel formation during the last 200,000 years, *Palaeogeogr. Palaeoclimatol.*, 157, 45–58, 2000.

Kallel, N., Paterne, M., Duplessy, J.-C., Vergnaud-Grazzini, C., Pujol, C., Labeyrie, L., Arnold, M., Fontugne, M., and Pierre, C.: Enhanced rainfall in the Mediterranean region during the last sapropel event, *Oceanol. Acta*, 20, 697–712, 2012.

Paleoclimate reconstruction in the Levant region

C. Nehme et al.

[Title Page](#)[Abstract](#)[Introduction](#)[Conclusions](#)[References](#)[Tables](#)[Figures](#)[Back](#)[Close](#)[Full Screen / Esc](#)[Printer-friendly Version](#)[Interactive Discussion](#)

- Kim, S. T. and O'Neil, J. R.: Equilibrium and nonequilibrium oxygen isotope effects in synthetic carbonates, *Geochim. Cosmochim. Ac.*, 61, 3461–3475, 1997.
- Kopp, R. E., Simons, F. J., Mitrovica, J. X., Maloof, A. C., and Oppenheimer, M.: Probabilistic assessment of sea level during the last interglacial stage, *Nature*, 462, 863–867, 2009.
- 5 Kolodny, Y., Stein, M., and Machlus, M.: Sea-rain-lake relation in the Last Glacial East Mediterranean revealed by $\delta^{18}\text{O}$ - $\delta^{13}\text{C}$ in Lake Lisan aragonites, *Geochim. Cosmochim. Ac.*, 69, 4055–4060, 2005.
- Lachniet, M. S.: Climatic and environmental controls on speleothem oxygen isotope values, *Quaternary Sci. Rev.*, 28, 412–432, 2009.
- 10 Lisker, S., Vaks, A., and Bar-Matthews, M.: Late Pleistocene palaeoclimatic and palaeoenvironmental reconstruction of the Dead Sea area (Israel), based on speleothems and cave stromatolites, *Quaternary Sci. Rev.*, 29, 1201–1211, 2010.
- Litt, T., Pickarski, N., Heumann, G., Stockhecke, M., and Tzedakis, P. C.: A 600 000 year long continental pollen record from Lake Van, eastern Anatolia (Turkey), *Quaternary Sci. Rev.*, 15 104, 30–41, 2014.
- Lourens, L. J., Antonarakou, A., Hilgren, F. J., Van Hoof, A. A. M., Vergnaud-Grazzini, C., and Zachariasse, W. J.: Evaluation of the Plio-Pleistocene astronomical timescale, *Paleoceanography*, 11, 391–413, 1996.
- McDermott, F.: Paleo-climate reconstruction from stable isotope variations in speleothems: a review, *Quaternary Sci. Rev.*, 23, 901–918, 2004.
- 20 Moller, T., Schultz, H., Hamann, Y., Dellwig, O., and Kucera, M.: Sedimentology and geochemistry of an exceptionally preserved last interglacial sapropel S5 in the Levantine Basin (Mediterranean Sea), *Mar. Geol.*, 291–294, 34–48, 2012.
- Otto-Bliesner, B. L., Marshall, S. J., Overpeck, J. T., Miller, G. H., Hu, A., and CAPE Last Interglacial Project members: Simulating Arctic climate warmth and icefield retreat in the Last Interglacial, *Science*, 311, 1751–1753, 2006.
- 25 Parton, A., White, T. S., Parker, A. G., Breeze, P. S., Jennings, R., Groucutt, H. S., and Petraglia, M. D.: Orbital-scale climate variability in Arabia as a potential motor for human dispersals, *Quatern. Int.*, doi:10.1016/j.quaint.2015.01.005, in press, 2015.
- 30 Petit-Maire, N., Carbonel, P., Reyss, J. L., Sanlaville, P., Abed, A., Bourrouilh, R., Fontugne, M., and Yasin, S.: A vast Eemian palaeolake in Southern Jordan (29° N), *Global Planet. Change*, 72, 368–373, doi:10.1016/j.gloplacha.2010.01.012, 2010.

Paleoclimate reconstruction in the Levant region

C. Nehme et al.

Title Page

Abstract

Introduction

Conclusions

References

Tables

Figures



Back

Close

Full Screen / Esc

Printer-friendly Version

Interactive Discussion



Rohling, E. J., Cane, T. R., Cooke, S., Sprovieri, M., Bouloubassi, I., Emeis, K. C., Schiebel, R., Kroon, D., Jorissen, F. J., Lorre, A., and Kemp, A. E. S.: African monsoon variability during the previous interglacial maximum, *Earth Planet. Sc. Lett.*, 202, 61–75, 2002.

Rosignol-Strick, M. and Panterre, M.: The Holocene climatic optimum and pollen records of sapropel 1 in the Eastern Mediterranean, 9000–6000 BP, *Quaternary. Sci. Rev.*, 18, 515–530, 1999.

Rozanski, K., Araguas, L., and Gonfiantini, R.: Isotopic patterns in modern global precipitation, in: *Climate Change in Continental Isotopic Record*, Geophysical Monograph Series, AGU, Washington DC, 78, 1–37, 1993.

Saad, Z., Slim, K., Ghaddar, A., Nasreddine, M., and Kattan, Z.: Composition chimique des eaux de pluie du Liban; Chemical composition of rain water in Lebanon, *Journal Europeen d'Hydrologie*, 31–2, 105–120, 2000.

Schmiedl, G., Mitschele, A., Beck, S., Emeis, K. C., Hemleben, Ch., Schultz, H., Sperling, M., and Weldeab, S.: Benthic foraminiferal record of ecosystem variability in the eastern Mediterranean Sea during times of sapropel S5 and S6 deposition, *Palaeogeogr. Palaeocl.*, 190, 139–164, 2003.

Scriver, A. E., Vance, D., and Rohling, E. J.: New neodymium isotope data quantify Nile involvement in Mediterranean anoxic episodes, *Geology*, 32, 565–568, 2004.

Shackleton, N. J., Chapman, M., Sanchez Goni, M. F., Pailler, D., and Lancelot, Y.: The classic marine isotope substage 5e, *Quaternary Res.*, 58, 14–16, 2002.

Stockhecke, M., Sturm, M., Brunner, I., Schmincke, H.-U., Sumita, M., Kipfer, R., Cukur, D., Kwiecien, O., and Anselmetti, F.: Sedimentary evolution and environmental history of Lake Van (Turkey) over the past 600 000 years, *Sedimentology*, 61, 1830–1861, 2014.

Vaks, A., Bar-Matthews, M., Ayalon, A., Schilman, B., Gilmour, M., Hawkesworth, C. J., Frumkin, A., Kaufman, A., and Matthews, A.: Paleoclimate reconstruction based on the timing of speleothem growth, oxygen and carbon isotope composition from a cave located in the “rain shadow”, Israel, *Quaternary Res.*, 59, 182–193, 2003.

Vaks, A., Bar-Matthews, M., Ayalon, A., Matthews, A., Frumkin, A., Dayan, U., Halicz, L., Almogi-Labin, A., and Schilman, B.: Paleoclimate and location of the border between Mediterranean climate region and the Saharo-Arabian desert as revealed by speleothems from the northern Negev Desert, Israel, *Earth Planet. Sc. Lett.*, 249, 384–399, 2006.

Paleoclimate reconstruction in the Levant region

C. Nehme et al.

Title Page

Abstract

Introduction

Conclusions

References

Tables

Figures



Back

Close

Full Screen / Esc

Printer-friendly Version

Interactive Discussion



Vaks, A., Bar-Matthews, M., Matthews, A., Ayalon, A., and Frumkin, A.: Middle-late quaternary paleoclimate of northern margins of the Saharan-Arabian Desert: reconstruction from speleothems of Negev Desert, Israel, *Quaternary Sci. Rev.*, 29, 2647–2662, 2013.

Verheyden, S., Nader, F. H., Cheng, H. J., Edwards, L. R., and Swennen, R.: Paleoclimate reconstruction in the Levant region from the geochemistry of a Holocene stalagmite from the Jeita cave, Lebanon, *Quaternary Res.*, 70, 368–381, 2008.

Waldmann, N., Stein, M., Ariztegui, D., and Starinsky, A.: Stratigraphy, depositional environments and level reconstruction of the last interglacial Lake Samra in the Dead Sea basin, *Quaternary Res.*, 72, 1–15, 2009.

Wang, Y. J., Cheng, H., Edwards, R. L., An, Z. S., Wu, J. Y., Shen, C. C., and Dorale, J. A.: A high-resolution absolute-dated Late Pleistocene monsoon record from Hulu cave, China, *Science*, 294, 2345–2348, 2001.

World Bank: Republic of Lebanon: Policy note on irrigation sector sustainability, Report No. 28766-LE. The World Bank, Washington DC, 2003.

Zanchetta, G., Drysdale, R. N., Hellstrom, J. C., Fallick, A. E., Isola, I., Gaganf, M. K., and Pareschi, M. T.: Enhanced rainfall in the Western Mediterranean during deposition of sapropel S1: stalagmite evidence from Corchia cave (Central Italy), *Quaternary Sci. Rev.*, 26, 279–286, 2007.

Ziegler, M., Tuenter, E., and Lourens, L. J.: The precession phase of the boreal summer monsoon as viewed from the eastern Mediterranean (ODP Site 968), *Quaternary Sci. Rev.*, 29, 1481–1490, 2010.

Paleoclimate reconstruction in the Levant region

C. Nehme et al.

Table 1. U–Th results of K1-2010 dating.

| Sample Number | Distance from base (cm) | U (ppm) | ²³² Th (ppb) | [²³⁰ Th/ ²³² Th] (measured) | [²³⁰ Th/ ²³⁸ U] (corrected) | [²³⁴ U/ ²³⁸ U] (corrected) | ρ_{08-48} uncorrected (ka) | Age corrected (ka) | Age corrected (ka) | Age BP ₁₉₅₀ | [²³⁴ U/ ²³⁸ U] _{initial} |
|---------------|-------------------------|---------|-------------------------|--|--|---|---------------------------------|--------------------|----------------------|------------------------|--|
| KA STM 1–4 | 2.4 | 0.1549 | 0.5079 | 520.1 | 0.5602 ± 0.27 | 0.8328 ± 0.13 | 0.07 | 129.92 ± 0.80 | 129.79 ± 0.80 | 129.72 ± 0.80 | 0.7588 ± 0.26 |
| KA STM 1–5 | 2.9 | 0.1425 | 1.623 | 147.2 | 0.5497 ± 0.37 | 0.8297 ± 0.18 | 0.47 | 126.47 ± 0.77 | 126.02 ± 0.83 | 125.96 ± 0.83 | 0.7570 ± 0.26 |
| KA STM 1–6 | 4.1 | 0.07508 | 3.488 | 37.5 | 0.5665 ± 1.0 | 0.8298 ± 0.56 | 0.85 | 135.85 ± 0.97 | 133.99 ± 1.63 | 133.93 ± 1.63 | 0.7515 ± 0.93 |
| KA STM 1–7 | 5.2 | 0.05155 | 1.207 | 74.1 | 0.5671 ± 0.59 | 0.8558 ± 0.31 | 0.67 | 125.46 ± 0.89 | 124.57 ± 1.08 | 124.51 ± 1.08 | 0.7950 ± 0.50 |
| KA STM 1–8 | 6.9 | 0.05426 | 2.676 | 35.1 | 0.5623 ± 1.1 | 0.8640 ± 0.59 | 0.82 | 121.74 ± 0.82 | 119.91 ± 1.53 | 119.84 ± 1.53 | 0.8092 ± 0.87 |
| KA STM 1–9 | 7.9 | 0.07067 | 0.8548 | 139.8 | 0.5541 ± 0.40 | 0.8809 ± 0.19 | 0.42 | 112.31 ± 0.68 | 111.88 ± 0.74 | 111.81 ± 0.74 | 0.8367 ± 0.24 |
| KA STM 1–2 | 8.8 | 0.06580 | 0.8400 | 124.6 | 0.5208 ± 0.51 | 0.8716 ± 0.31 | 0.26 | 103.03 ± 0.90 | 102.57 ± 0.96 | 102.50 ± 0.96 | 0.8284 ± 0.48 |
| KA STM 1–10 | 11.6 | 0.05592 | 0.7053 | 121.9 | 0.5037 ± 0.45 | 0.8579 ± 0.21 | 0.44 | 100.41 ± 0.61 | 99.94 ± 0.69 | 99.88 ± 0.69 | 0.8116 ± 0.25 |
| KA STM 1–11 | 13.5 | 0.07340 | 0.2089 | 516.7 | 0.4829 ± 0.30 | 0.8532 ± 0.13 | 0.06 | 94.27 ± 0.50 | 94.16 ± 0.51 | 94.10 ± 0.51 | 0.8085 ± 0.25 |
| KA STM 1–3 | 19.5 | 0.05971 | 0.7545 | 108.5 | 0.4486 ± 0.56 | 0.8439 ± 0.33 | 0.27 | 85.83 ± 0.70 | 85.36 ± 0.78 | 85.30 ± 0.78 | 0.8014 ± 0.50 |

Uncertainties for activity ratios and ages are $\pm 2\sigma$ (%) and $\pm 2\sigma$ (ka), respectively. ²³⁰Th and ²³⁴U decay constants are from Cheng et al. (2013); the ²³⁸U decay constant is from Jaffey et al. (1971). Detrital Th corrections assumed an initial ²³⁰Th/²³²Th atomic ratio = $4.4 \times 10^{-6} \pm 50\%$ and a bulk earth ²³²Th/²³⁸U of 3.8.

Title Page

Abstract

Introduction

Conclusions

References

Tables

Figures



Back

Close

Full Screen / Esc

Printer-friendly Version

Interactive Discussion



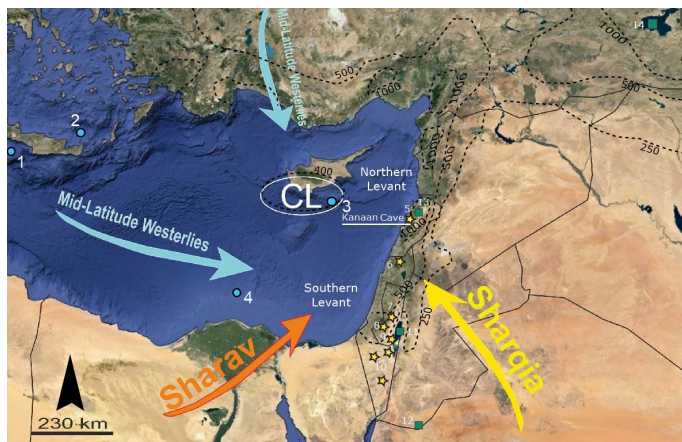


Figure 1. The Eastern Mediterranean showing the location of palaeoclimate records including this study and the major wind trajectories (Saaroni et al., 1998), including the Mid-Latitude Westerlies, and occasional incursions from the Sharav cyclone and the Sharqiya. The north–south and east–west precipitation gradients are indicated by dashed dark lines (isohyets in mm). CL: Cyprus Low. The location of Kanaan Cave and other Levantine paleoclimatic records spanning the MIS 5 period cited in the text, are numbered 1 to 14. Records derived from marine studies are indicated by points, lake level reconstructions and pollen data by rectangles and speleothems by stars. (1) Core MD 70-41 (Emeis et al., 2003), (2) Core LC21 (Grant et al., 2012), (3) Core ODP site 967 (Emeis et al., 2003; Rohling et al., 2002, 2004; Scrivner et al., 2004), (4) Core ODP site 968 (Ziegler et al., 2010), (5) Kanaan Cave, (6) Peqiin Cave (Bar-Mathews et al., 2003), (7) West Jerusalem Cave (Frumkin et al., 1999, 2000), (8) Soreq Cave (Bar-Mathews et al., 2000, 2003) (9) Tsavoa Cave (Vaks et al., 2006, 2013), (10) Negev composite speleothems from Ashalim, Hol-Zakh and Ma’ale-ha-Meyshar caves (Vaks et al., 2013), (11) Lakes of the Dead Sea basin (Kolodny et al., 2005; Waldmann et al., 2009; Lisker et al., 2010), (12) Lake formation at Mudawwara (Petit-Maire et al., 2010); (13) Yammouneh Paleolake (Develle et al., 2011; Gasse et al., 2011, 2014), (14) Lake Van (Shtokhete et al., 2014; Litt et al., 2014).

Paleoclimate reconstruction in the Levant region

C. Nehme et al.

Title Page

Abstract

Introduction

Conclusions

References

Tables

Figures



Back

Close

Full Screen / Esc

Printer-friendly Version

Interactive Discussion



Paleoclimate reconstruction in the Levant region

C. Nehme et al.

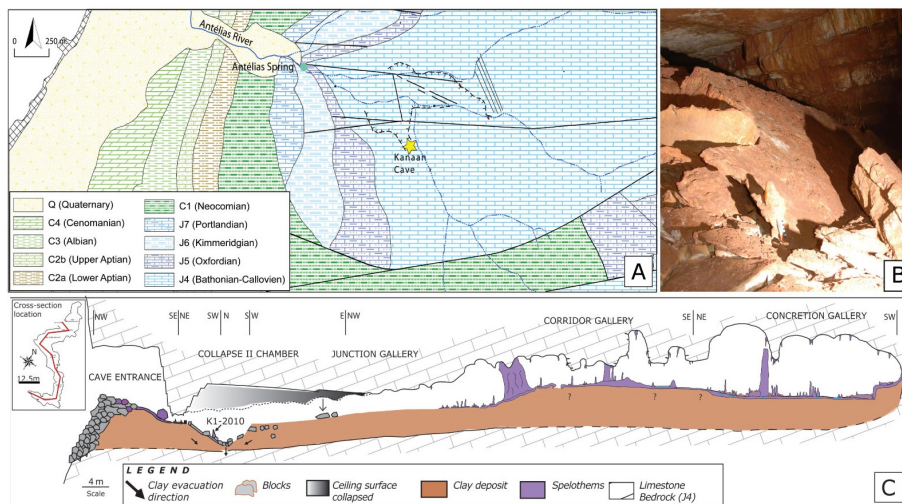


Figure 2. (a) Location map of Kanaan cave and the continental records in the Levant. (a) Geological map of the Antelias region (western flank of central Mount-Lebanon) (Dubertret, 1955). (b) Photo of K1-2010 stalagmite in the Collapse Chamber (c) Geomorphological section of Kanaan Cave showing the location of the stalagmite K1-2010 (Nehme, 2013).

Title Page

Abstract

Introduction

Conclusions

References

Tables

Figures



Back

Close

Full Screen / Esc

Printer-friendly Version

Interactive Discussion



Stalagmite K1-2010 (Kanaan cave)

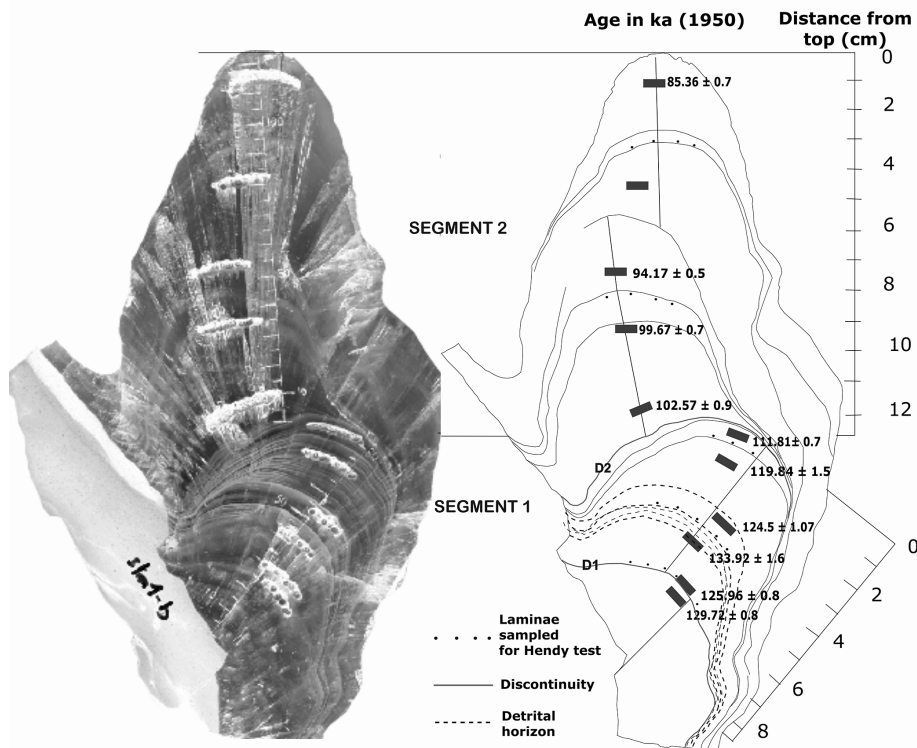


Figure 3. Cut face of the K1-2010 speleothem and sketch showing the position of the Uranium series age data. In Segment 1, the dashed line indicates detrital layers and U/Th shows much more uncertainties than those in the Segment 2. The third age from the base of the segment 1 is an outlier. Segment 1 is tilted from its initial position probably due to the suffusion of clay deposits in the Collapse Chamber that caused the block on which the speleothem grew to subside. D1 and D2 indicate discontinuities.

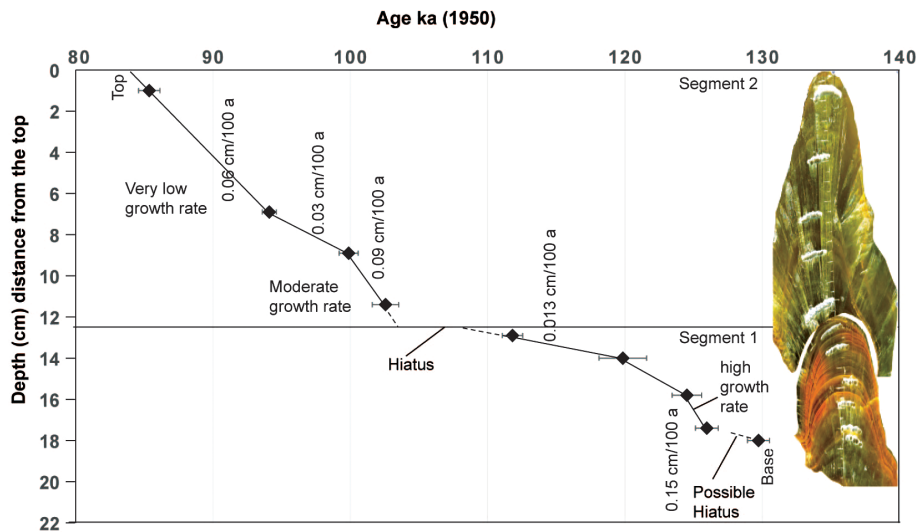


Figure 4. Growth rate of the stalagmite with respect to distance (in mm) from the top, assuming linear growth rates between two consecutive dates except in the middle part where a discontinuity (hiatus) is identified.

Paleoclimate reconstruction in the Levant region

C. Nehme et al.

Title Page

Abstract Introduction

Conclusions References

Tables Figures

◀ ▶

◀ ▶

Back Close

Full Screen / Esc

Printer-friendly Version

Interactive Discussion



Paleoclimate
reconstruction in the
Levant region

C. Nehme et al.

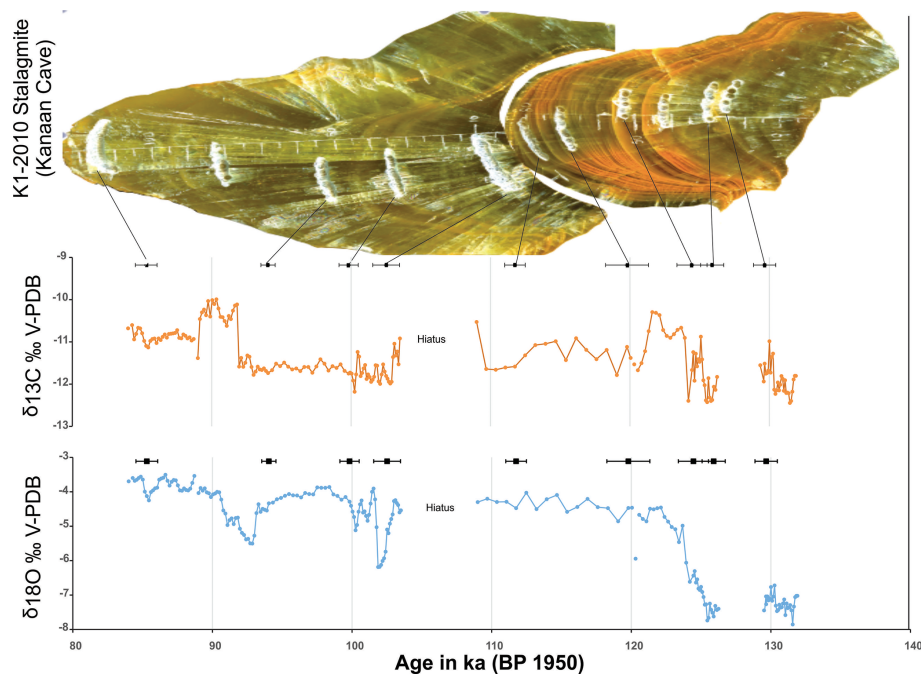


Figure 5. $\delta^{18}\text{O}$ and $\delta^{13}\text{C}$ profiles (values are in ‰ VPDB) of samples microdrilled along the growth axis of the K1-2010 stalagmite (Kanaan cave, Lebanon).

Title Page

Abstract

Introduction

Conclusions

References

Tables

Figures



Back

Close

Full Screen / Esc

Printer-friendly Version

Interactive Discussion



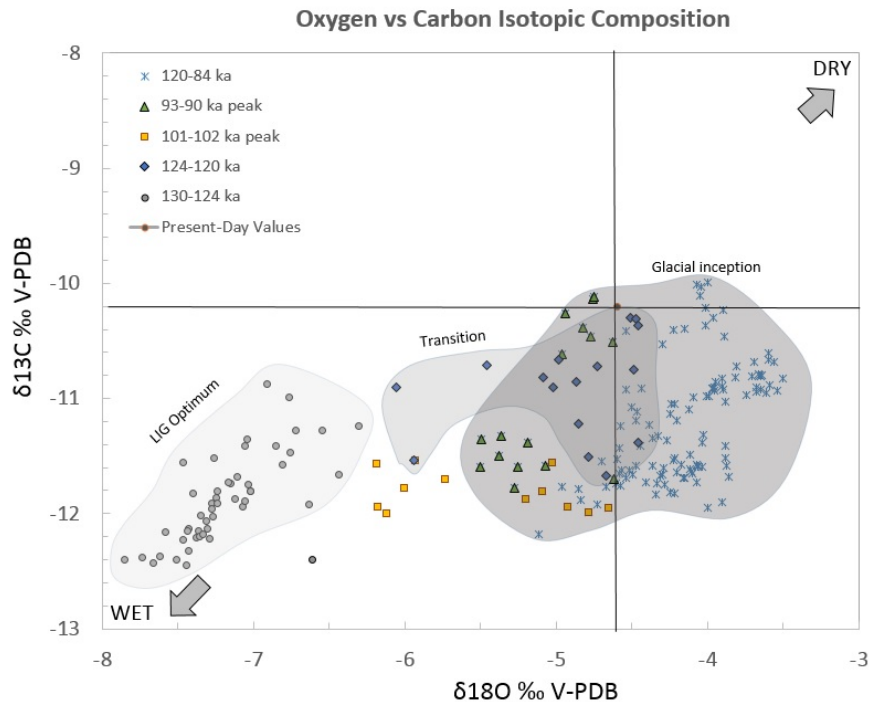


Figure 6. Oxygen vs. carbon stable isotopic composition (values are in ‰ V-PDB) of samples microdrilled along the growth axis of the K1-2010 stalagmite (Kanaan cave, Lebanon). The present-day $\delta^{18}\text{O}$ value for the precipitated calcite was calculated using the Kim and O’Neil (1997) equilibrium equation. The $\delta^{13}\text{C}$ value was obtained from the Holocene $\delta^{13}\text{C}$ mean value of Jeita cave (Verheyden et al., 2008). This cave, located just 20 km to the north has very similar climate, vegetation geology, soil type, and altitude (98 ma.s.l.) to Kanaan Cave.

| | |
|--------------------------|--------------|
| Title Page | |
| Abstract | Introduction |
| Conclusions | References |
| Tables | Figures |
| ◀ | ▶ |
| ◀ | ▶ |
| Back | Close |
| Full Screen / Esc | |
| Printer-friendly Version | |
| Interactive Discussion | |



Paleoclimate reconstruction in the Levant region

C. Nehme et al.

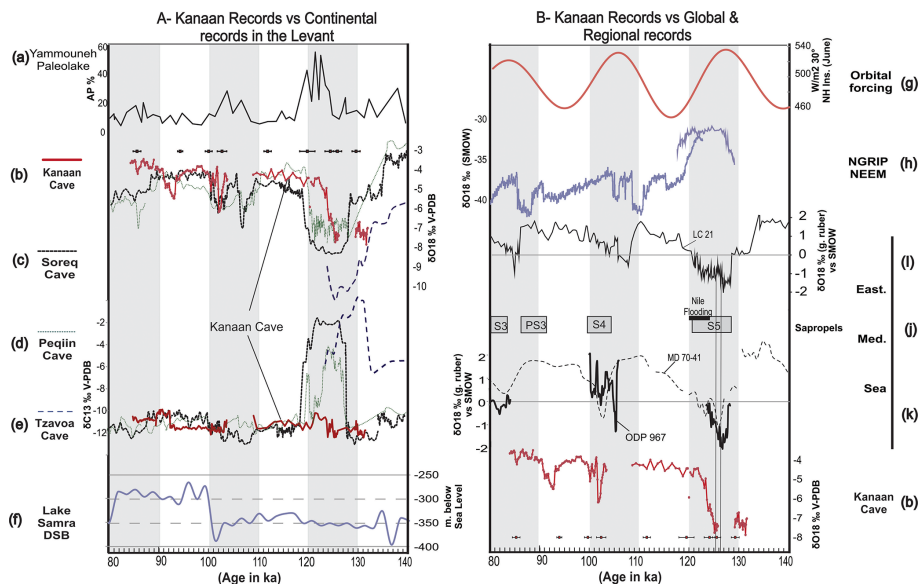


Figure 7. A – Kanaan Cave $\delta^{18}\text{O}$ and $\delta^{13}\text{C}$ profiles compared to continental records in the Levant. From North to South Levant: (a) Yammouneh AP %, north Lebanon (Gasse et al., 2015), (b) Kanaan carbon and oxygen isotopic profile (this study), (c) Soreq Cave, (d) Peqin Cave (Bar-Mathews et al., 2000, 2003), (e) Tzavoa Cave (Vaks et al., 2006), (f) lake Samra paleolevels in the Dead Sea Basin (Waldmann et al., 2009). B – Kanaan Cave $\delta^{18}\text{O}$ profile compared to global and regional records in the Eastern Mediterranean Basin: (g) Summer insolation at 30° N and orbital eccentricity forcing (Berger and Loutre, 1991), (h) NGRIP-NEEM indicating the volume of the arctic Ice sheet (NGRIP team, 2004), (i) Eastern Mediterranean $\delta^{18}\text{O}_{\text{G.ruber}}$ in core LC21 (Grant et al., 2012), (j) Mediterranean sapropel events (Ziegler et al., 2010) and the Nile flooding event (Scrivner et al., 2004), (l) EMS Mediterranean $\delta^{18}\text{O}_{\text{G.ruber}}$ in ODP site 967 and in MD 70-41 site resampled at 1 ka interval (Emeis et al., 2003).

Title Page

Abstract

Introduction

Conclusions

References

Tables

Figures



Back

Close

Full Screen / Esc

Printer-friendly Version

Interactive Discussion

